Available online at www.sciencedirect.com

ScienceDirect

Procedia Structural Integrity 15 (2019) 67–74

Structural Integrity Procedia

www.elsevier.com/locate/procedia

International Conference on Stents: Materials, Mechanics and Manufacturing ICS3M 2019

A Computational Modelling of the Mechanical Performance of a Bioabsorbable Stent Undergoing Cyclic Loading

Xinyang Cui[a], Kun Peng[a], Sicong Liu[a], Qingshuai Ren[a,b], Gaoyang Li[a,c] , Zhaoyong Gu[a], Aike Qiao[a,]*

[a]*College of Life Science and Bioengineering, Beijing University of Technology, No.100, Pingleyuan, Chaoyang District, Beijing, 100022,China.*
[b] *Institute of Mechanics, Chinese Academy of Science, No.15, BeiSiHuanWest Road, Beijing, 100190, China.*
[c] *Graduate School of Biomedical Engineering, Tohoku University, Sendai, Miyagi, 980-8577, Japan*

Abstract

In order to address new challenges that arise in the degradation behavior of absorbable metal stents (AMSs) *in vivo*, new modelling and simulation are presented in this study. A dynamic corrosion model (Model 1) considering uniform corrosion, stress corrosion mechanisms and dynamic cyclic pulse loading was proposed to simulate the stent degradation based on Continuum Damage Mechanics (CDM). A control group (Model 2) was established which only considered the mechanisms of uniform and stress corrosion. The time of stent degraded completely in Model 1 was set as a normalized time unit (100t) to illustrate the results. With the increase of time, the mass and supporting performance of the stent decreased, especially at 10t to 20t. The average von Mises Stress of the stent in the Model 1 decreases from 86.19 MPa to 48.65 MPa roughly at 5t to15t, while the average von Mises Stress in Model 2 decreases from 87.12 MPa to 50 MPa. The mass loss ratio of stents in Model 1 is always higher than that in Model 2, and the relative error of the mass loss ratio reached 14.3% at 20t. The results showed that the corrosion occurs at first in the stent struts with the highest von Mises stress. In addition, the dynamic cyclic pulse loading accelerated the degradation rate and the supporting performance loss of stent. These modelling and simulation techniques may provide new insights to *in vivo* AMS performance.

* Corresponding author. Tel.: +81-10-67396657; fax: +81-10-67396657.
E-mail address: qak@bjut.edu.cn

2452-3216
10.1016/j.prostr.2019.07.013

Keywords: Finite element analysis; Absorbable stent; Corrosion modelling; Biomechanics

1. Introduction

Bioabsorbable intravascular stents have gained attention to treat the artery disease in recent years since they can perform a mechanical support to the artery for a scaffolding period (6-12 months) and then be absorbed by the body. This characteristic is not only suitable for adult patients but also benefit for the growing vessels of paediatric patients (Zartner et al., 2005; Schranz et al., 2006; Wykrzykowska et al., 2009), and can avoid long-term complications (Köster et al., 2000; Virmani et al., 2004), reduce risk of in-stent restenosis [Mitra, 2006; Hoffmann et al., 1996] and late stent thrombosis (Morlacchi et al., 2014).

A bioabsorbable stent is supposed to disappear completely after the scaffolding time is complete and the arterial wall has remodelled. In this certain scaffolding period, the bioabsorbable materials, such as metallic alloys (ferroalloy, magnesium alloy, zinc alloy, etc.) have many chemical and physical reactions. As reviewed by Boland et.al, the description of corrosion mechanism of metal alloys generally includes but not limited to micro-galvanic corrosion, pitting corrosion and intergranular corrosion, stress corrosion cracking (SCC) and corrosion fatigue.

Taking a zinc alloy stent as an example, firstly, the zinc alloy is highly susceptible to micro-galvanic corrosion. In in vivo corrosion environment, the metal zinc acts as anode, alloy element or impurity acts cathode, and localized pitting corrosion occurs at the cathode. After the crimped stent expanded the stenotic vessel to a healthy diameter, the interaction between the residual stress and the blood environment can lead to SCC. More attention should be paid to SCC because it can lead to stent fast fracture (Morlacchi et al., 2014; Auricchio et al., 2015), eventually cause an in-stent restenosis (Shaikh et al., 2008; Adlakha et al., 2010). During the stent service period, the blood flow induced pulsatile pressure acts on the inner surface of the blood vessel. The corrosion fatigue of stent is caused by the combined action of an alternating stress or the pulsatile stress and the blood aggressive environment. In the degradation process, the stent structure damages and the material mechanical properties weakening occur simultaneously and interact with each other. In the meanwhile, the interaction between the stent and the blood vessels also keeps changing until the stent degrades completely (Grogan et al., 2013).

Finite element analysis (FEA) has been a valuable tool for accounting for corrosion modelling. Based on Continuum Damage Mechanics (CDM), a number of numerical models for micro-galvanic and pitting corrosion have been proposed (Wu et al., 2011; Grogan et al., 2014) to predict the corrosion rate. Wu et al. developed the coupled formulation of uniform micro-galvanic corrosion and stress corrosion to optimize the mechanical performances of the absorbable stent. The influence of aggressive environment and a cyclic pulse stress on the corrosion fatigue was studied by tests under different corrosive environments (Bhuiyan et al., 2008; Nan et al., 2008; Boland et al., 2016). The corrosion fatigue behavior under *in vivo* condition is still a hard challenge, especially capturing the effects of the in vivo environment (cyclic pulsatile loading) on the rates of corrosion with computation technique (Winzer et al., 2005).

2. Methodology

2.1. Geometry models and material properties

Bioabsorbable zinc alloy was selected as the stent material due to its combination of mechanical properties and biocompatibility. The zinc alloy in this paper was consisted of Zn, Mg, Al, and the true strain-stress curves of this zinc alloy was shown in Fig.1. The zinc alloy has a modulus of 98 GPa, Poisson's ratio of 0.30, density of 6.7 g/mm^3, a yield stress of 220 MPa, and ultimate tensile strength of 325 MPa, and it was modelled as a homogeneous, isotropic, elastoplastic material. To save the simulation time, only one stent ring consisted of 10 crowns was chosen for the degradation model. The dimension details were shown in Fig. 2. The artery vessel property used in this paper is identical to that used in our previous studies (Cui et al., 2018a; Cui et al., 2018b). The combination of the stent and the artery were meshed with the C3D8R using the software Hypermesh 11.0.

To investigate the influence of cyclic pulsatile loading on the stent degradation behavior, a dynamic corrosion model (named Model 1) was established where not only two corrosion mechanisms was considered, but also the

influence of dynamic cyclic pulsatile loading on corrosion behaviour was taken into account. In addition, a control group (named Model 2) considering only two corrosion mechanisms was established.

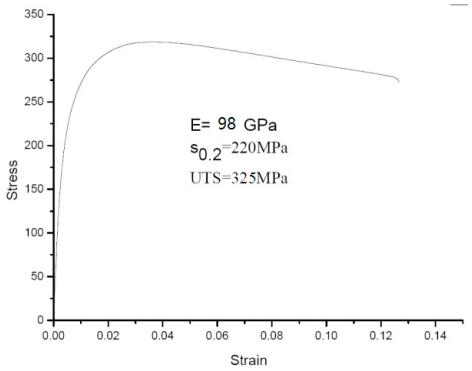

Fig. 1. True strain-stress curves of the zinc alloy.

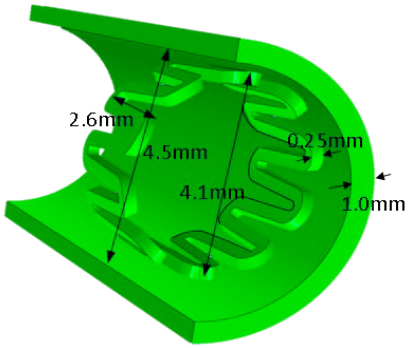

Fig. 2. Geometrical dimensions of the stent and artery.

Two simulation steps were executed for the whole simulation.

Step 1: stent crimping-expansion. In order to simulate crimping of the stent on a balloon catheter, a displacement load corresponding to a diameter of 15% was assigned. Subsequently, the stent was delivered to the stenotic lesion. A uniform radial deformation, up to a diameter of 1.1 times of the healthy vessel inner diameter, was imposed on the inner surface of the carotid stent along the longitudinal axis (Dordoni et al., 2014). At the end of this step, the stent was deflated and the vessel wall elastically recoiled.

In this step, the corrosion procedure was not taken into account, and this process was simulated using ABAQUS/Standard solver.

Step 2: the whole model and its mechanical results after the step 1 were imported into the corrosive environment. This approach was implemented in ABAQUS/Explicit through user subroutines VUSDFLD. A flowchart outlining the operation of the corrosion model was shown in Fig. 3. After subjecting the stent to a large deformation in step 1, the stent underwent pulsatile loading produced from the oscillation of the internal blood pressure. To simulate the blood cyclic pulsatile loading effects on the stent degradation, the pulsatile pressure that changes over time was applied to the inner surface of the vessel. The stent began to degrade in corrosive environment similar to in vivo situation.

2.2. Establishment of corrosion degradation model

Based on continuous damage mechanics, a corrosion model of zinc alloy was established where the uniform

current corrosion and stress corrosion cracking (SCC)) were taken into account. With regards to the isotropic damage hypothesis, the continuous damage model sets the damage field D by defining a continuous function related to time and boundary conditions, so as to simulate the reduction of macroscopic mechanical properties (such as stiffness, yield stress, etc.) of the material. The effective stress during the damage process can be calculated as shown in Equation (1),

$$\sigma = （1 - \mathrm{D}）\overline{\sigma} \tag{1}$$

where σ means the effective stress, $\overline{\sigma}$ is the undamaged stress, D is a damage variable which increases monotonously from 0 to 1. There is not any damage in the material if D is equal to 0, while D= 1 means the material completely lost its capability.

Considering the uniform micro-current corrosion and stress corrosion which caused the overall degradation of the stent, D is assumed to be linear superposition of the uniform corrosion damage D_U and the stress corrosion damageD_{SC}, as shown in Equation (2),

$$\mathrm{D} = D_U + D_{SC} \tag{2}$$

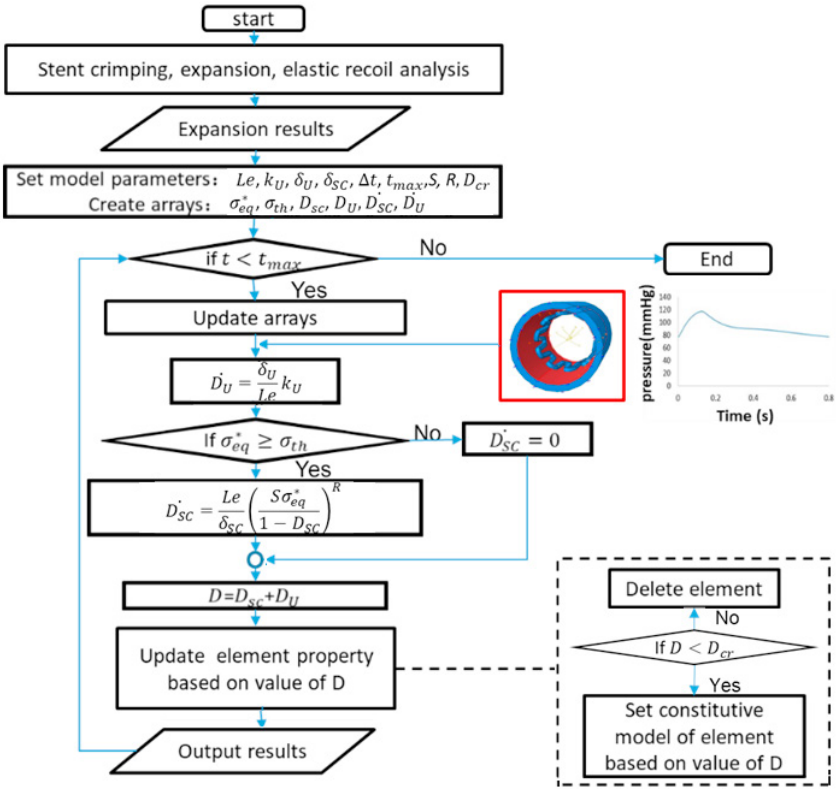

Fig. 3. Simplified flowchart of the corrosion model process.

The uniform corrosion damage D_U is defined to describe the mass loss of material when the material is exposed in aggressive environment. The damage evolution law of uniform corrosion process is supposed to be functions of δ_U, k_U and L_e with the following form of equation (3).

$$\dot{D}_U = \frac{\delta_U}{L_e} k_U \tag{3}$$

where k_U is a parameter related to the kinetics of the uniform corrosion process, δ_U is a characteristic dimension of the uniform corrosion process, and L_e is the characteristic length of a finite element. In Gastaldi's research, the value of k_U is between 0.01/h and 0.1/h (Gastaldi et al., 2011). Based on the immersion test completed in our research, the details of uniform corrosion dynamic parameters are listed in Table 1.

The D_{SC} represents the damage associated with stress corrosion cracking (SCC) processes. Stress corrosion cracking model can be established, as shown in equation (4) and equation (5).

$$\dot{D}_{SC} = 0 \qquad \sigma_{eq}^{*} < \sigma_{th} \tag{4}$$

$$\dot{D}_{SC} = \frac{L_e}{\delta_{sc}}\left(\frac{S\sigma_{eq}^{*}}{1-D}\right)^{R} \qquad \sigma_{eq}^{*} \geq \sigma_{th} > 0 \tag{5}$$

where σ_{eq}^{*} is the equivalent Mises stress causing the stress corrosion of the stent, L_e is Element feature size in finite element analysis, m. δ_{SC} means the characteristic size of the stress corrosion process, m. σ_{th} is the stress threshold, closely related (Winzer et al., 2005) to the combination of material composition, metallurgical conditions and corrosive environment, and is set to 50% of the yield stress of zinc alloy, 110 MPa. S and R relate to the kinetics of the stress corrosion process, are a function of the corrosive environment. Based on the Costa-Mattos' research (Costa-Mattos et al., 2008), S and R are kept constant because a constant pH is adopted for the corrosive environment, the details of these relevant parameters are listed in Table 1.

Table 1 Parameters for the material degradation model.

Parameters	δ_U	k_U	δ_{SC}	σ_{th}	S	R
value	0.1mm	0.05/h	0.07mm	110MPa	0.005mm$^2\sqrt{\text{h}}$/N	2

The material degradation model is implemented into a finite element framework using the commercial code ABAQUS/Explicit 6.13 (ABAQUS Inc., USA) by means of a user subroutine (VUSDFLD). For beginning and evolution of the corrosion, the stress state is calculated and updated in the explicit time integration. In addition, the simplified flowchart of the corrosion model process is shown in Fig. 3.

The corrosion model considering the influence of the dynamic load of the blood flow pulsatile pressure is set to Model 1, in which the stent is implanted into the blood environment and which is set as the start time of 0, and the time for the complete degradation of the stent is set as 100 Time Unit (100t). The degradation of the stents in the two models was compared.

3. Results and discussion

The influence of pulsatile pressure on the degradation rate of stent will be discussed as follows.

(1) The mass loss ratio was selected as an evaluation index to compare the degradation rates in these two models. The volume of the stents at the time t (V_t) during the degradation process can been extracted from the finite element simulation results, and the material density (ρ) was assumed to be constant. Based on these, the approximate mess of the stent during the degradation process at the time t can be calculated as $\mathrm{M_t}=\rho V_t$. The calculation formula of mass loss ratios of stents was shown in equation (6) and the results were shown in Fig. 4.

$$\gamma = \frac{M_{\text{initial}} - \mathrm{M_t}}{M_{\text{initial}}} \tag{6}$$

where M_{initial} means the initial mess of the stent when it was not degraded; $\mathrm{M_t}$ means the approximate mess of the stent at the time t.

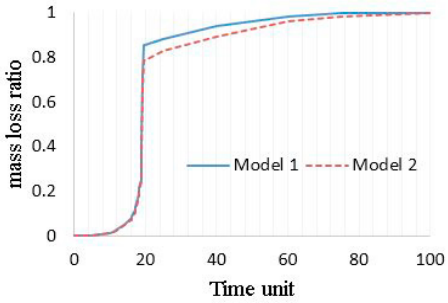

Fig. 4. Comparison of mass loss ratios of stents in degradation models.

(2) The structure of the stents changed with time during the degradation was shown in Fig. 5, and the damage condition of the stents can be compared using these damage contours.

(3) The average value of the von Mises Stress during the degradation process of the stent was selected to evaluate the influence of the dynamic load of the blood flow pulsatile blood pressure on the mechanical properties during the degradation process of the stent, as shown in Fig. 6.

In Fig. 4, quantitative comparison shows that the difference in mass loss ratio of the stent in the two degradation models is not obvious. Especially before 5t, the corrosion degradation of the stent hardly occurs and the mass loss ratio of the stent is small. During the degradation process, the mass loss ratio has positively correlation with time. The mass loss ratio of the stent begins to change within 5t-20t. After 10t, the stent degradation accelerates, and the growth of the mass loss ratio increases obviously. The mass loss ratios of stents in Model 1 is always higher than that in Model 2, and the relative error of the mass loss ratio reached 14.3% when t=20. Until 20t, the mass loss ratio in model 1 is larger than 0.80, which indicates that a large-area of stent structure fracture results in the rapid quality decrease. After this time, the difference of the mass loss ratios of stents in two models is obvious. This indicates that the blood flow pulsatile pressure promotes the degradation of the stent. It is necessary to pay attention on the degradation of the stent structure and the support performance of the stent during 5t to 20t.

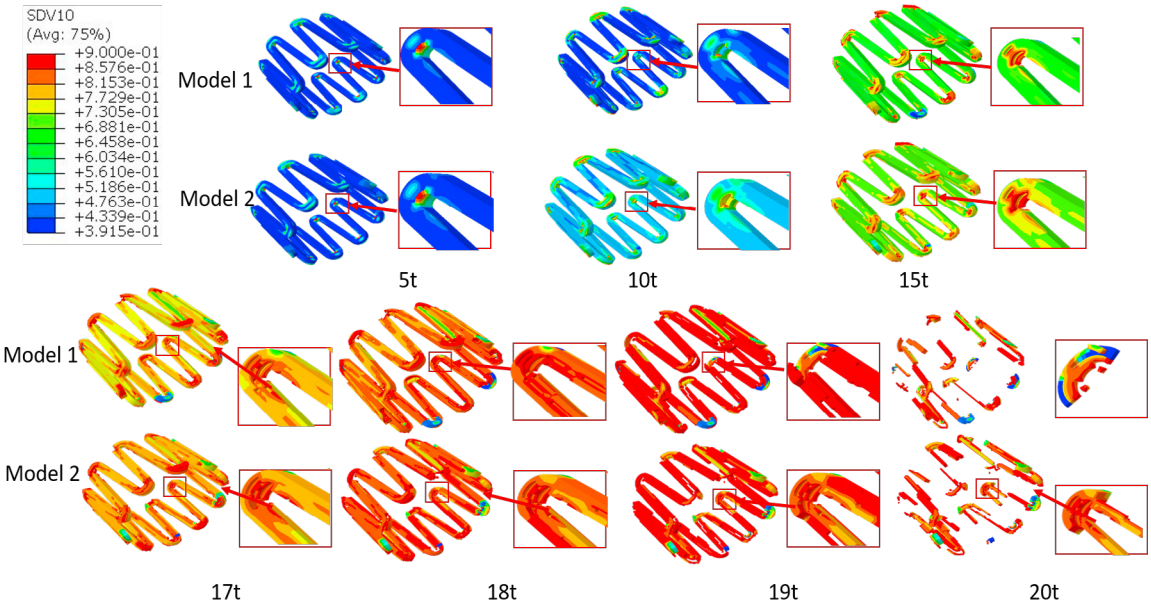

Fig. 5. Corrosion contour and structural damage comparison of the stents in the two models.

As shown in Fig. 5, compared to the corrosion contour and structural damage of the stents in the two models, the stents showed no damage in the two models before 5t. At this time, the corrosion factor contour is very similar. As can be seen from the corrosion contour, the element deletion occurs first at the inner surface of the bend in the stent crown, where the residual stress generated in the crimping-expansion process is much higher. The residual stress is the cause of the SCC. After 10t, the corrosion factor of in Model 1 is always higher than that in the Model 2. It indicates that the blood flow pulsation pressure has no significant effect on the initial cracking time of the stent, but once the stent cracked, the dynamic load of blood flow pulsatile pressure significantly accelerates the process from the cracking to the end of degradation. As shown in Fig.5, the changing rate of the stent damage and degradation under the effect of blood flow pulsatile pressure is higher than that without the influence of pulsatile dynamic pressure.

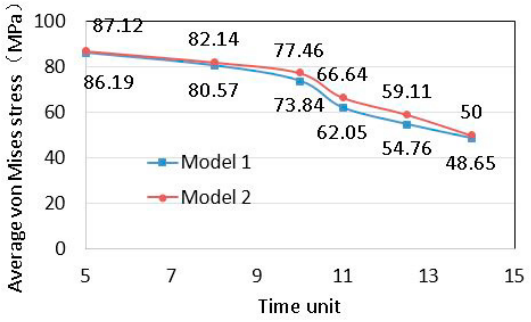

Fig. 6. Average von Mises stress of stents at 5t-15t.

The decrease of the average von Mises Stress represents the reduction of the support performance of the entire stent structure. The average equivalent stress of the stent during degradation from 5t to 15t is statistically calculated, as shown in Fig. 6. The average von Mises Stress of the stent in the Model 1 decreases from 86.19 MPa to 48.65 MPa roughly at 5t to15t, while the average von Mises Stress in Model 2 decreases from 87.12 MPa to 50 MPa. At 15 t, the average von Mises Stress of the stent is smaller than the threshold of stress corrosion, and the effect of stress corrosion cracking decreases over time. With the increase of degradation time, the stent degrades under the action of uniform corrosion and blood pulsatile pressure, and the degradation rate becomes slow. This is also the reason why the mass loss ratio in Fig. 4 decreases after 20t, and the support performance of the stent continues to be lost. Quantitative comparison shows that the stress distribution in Model 1 is slightly lower than that in Model 2, indicating that the support performance of the stent in Model 1 is lost faster than in Model 2 at the same time. This indicates that the blood flow pulsatile pressure dynamic load accelerates the loss of the support performance of the stent.

4. Conclusions

In the degradation process, the evolution of material degradation leads to a continuous weakening of stent structure and supporting properties. At the initial period of stent degradation, the stress corrosion plays a great rule in the corrosion of stent. The main influencing factor of the initial cracking of the stent is the residual stress after the stent expanded; the corrosion cracking occurs at first in the stent struts with the highest von Mises stress.

In the corrosive environment, once the stent is cracked, it would accelerate the degradation rate of the stent and the loss of the mechanical properties even the dynamic pressure of the blood flow is very small. Cyclic pulsatile loading has strong influence on the degradation behavior and the mechanical performance of stent. The established computational modelling of stent undergoing cyclic loading will contribute to a more proper mechanical analysis of bioabsorbable stents.

Acknowledgements

This work was supported by Major Project of Science and Technology of Beijing Municipal Education Commission and Type B Project of Beijing Natural Science Foundation (KZ201710005007).

References

Adlakha, S., Sheikh, M., Wu, J., Burket, M. W., Pandya, U., Colyer, W., Eltahawy, E., Cooper, C. J., 2010. Stent Fracture in the Coronary and Peripheral Arteries. Journal of Interventional Cardiology 23, 411-419.

Auricchio, F., Constantinescu, A., Conti, M., Scalet, G., 2015. Fatigue of Metallic Stents: from Clinical Evidence to Computational Analysis. Annals of Biomedical Engineering 44, 1-15.

Bhuiyan, M.S., Mutoh, Y., Murai, T., Iwakami, S., 2008. Corrosion Fatigue Behavior of Extruded Magnesium Alloy AZ61 under Three Different Corrosive Environments. International Journal of Fatigue 30, 1756-1765.

Boland, E. L., Shine, R., Kelly, N., Sweeney, C.A., Mchugh, P.E., 2016. A Review of Material Degradation Modelling for the Analysis and Design of Bioabsorbable Stents. Annals of Biomedical Engineering 44, 341-356.

Cui, X., Ren, Q., Li, G., Li, Z., Qiao, A., 2018a. Influence of the Realistic Artery Geometry Parameters on a Coronary Stent Fatigue Life. International Journal of Computational Methods, 1842006.

Cui, X., Ren, Q., Li, Z., Peng, K., Li, G., Gu, Z., Qiao, A., 2018b. Effect of Plaque Composition on Biomechanical Performance of a Carotid Stent: Computational Study. Computer Modeling in Engineering and Sciences 116, 455-469

Costa-Mattos H.S. D., Bastos I.N., Gomes J.A.C.P., 2008. A Simple Model for Slow Strain Rate and Constant Load Corrosion Tests of Austenitic Stainless Steel in Acid Aqueous Solution Containing Sodium Chloride. Corrosion Science 50, 2858-2866.

Dordoni, E., Meoli, A., Wu, W., Dubini, G., Migliavacca, F., Pennati, G., Petrini, L., 2014. Fatigue Behaviour of Nitinol Peripheral Stents: The Role of Plaque Shape Studied with Computational Structural Analyses. Medical Engineering and Physics 36, 842-849.

Gastaldi, D., Sassi, V., Petrini, L., Vedani, M., Trasatti, S., Migliavacca, F., 2011. Continuum Damage Model for Bioresorbable Magnesium Alloy Devices - Application to Coronary Stents. Journal of the Mechanical Behavior of Biomedical Materials 4, 352-365.

Grogan, J. A., Leen, S.B., Mchugh, P.E., 2013. Optimizing the Design of a Bioabsorbable Metal Stent using Computer Simulation Methods. Biomaterials 34, 8049-8060.

Grogan, J.A., Leen, S.B., Mchugh, P.E., 2014. A Physical Corrosion Model for Bioabsorbable Metal Stents. Acta Biomaterialia 10, 2313-2322.

Hoffmann, R., Mintz, G.S., Dussaillant, G.R., Popma, J.J., Pichard, A.D., Salter L.F., Kent, K.M., Griffin, J., Leon, M.B., 1996. Patterns and Mechanisms of In-Stent Restenosis: a Serial Intravascular Ultrasound Study. Circulation 94, 1247.

Mitra, A. K., 2006. In stent restenosis: bane of the stent era. Journal of Clinical Pathology, 59(3), 232-239.

Morlacchi, S., Pennati, G., Petrini, L., Dubini, G., Migliavacca, F., 2014. Influence of Plaque Calcifications on Coronary Stent Fracture: a Numerical Fatigue Life Analysis including Cardiac Wall Movement. Journal of Biomechanics 47, 899-907.

Nan, Z.Y., Ishihara, S., Goshima, T., 2008. Corrosion Fatigue Behavior of Extruded Magnesium Alloy AZ31 in Sodium Chloride Solution. International Journal of Fatigue 30, 1181-1188.

Köster, R., Vieluf, D., Kiehn, M., Sommerauer, M., Kähler, J., Baldus, S., Meinertz, T., Hamm, C.W., 2000. Nickel Molybdenum Contact Allergies in Patients with Coronary In-Stent Restenosis. The Lancet 356, 1895-1897.

Schranz D., Zartner P., Michel-Behnke I, Akinturk H., 2006. Bioabsorbable Metal Stents for Percutaneous Treatment of Critical Recoarctation of the Aorta in a Newborn. Catheter Cardiovascular Intervention 67, 671–3.

Shaikh, F., Maddikunta, R., Djelmami-Hani, M., Solis, J., Bajwa, T., 2008. Stent Fracture, an Incidental Finding or a Significant Marker of Clinical In-Stent Restenosis?. Catheterization and Cardiovascular Interventions 71, 614-618.

Virmani, R., Guagliumi G., Farb A., 2004. Localized Hypersensitivity and Late Coronary Thrombosis Secondary to a Sirolimus-Eluting Stent: Should We Be Cautious?. Circulation 109, 701-705.

Winzer, N., Atrens, A., Song, G.L., Ghali, E., Dietzel, W., Kainer, K.U., Hort, N., Blawert, C., 2005. A critical review of the stress corrosion cracking (SCC) of magnesium alloys. Adv. Eng. Mater. 7, 659–693.

Wu, W., Gastaldi, D., Yang, K., Tan, L., Petrini, L., Migliavacca, F., 2011. Finite Element Analyses for Design Evaluation of Biodegradable Magnesium Alloy Stents in Arterial Vessels. Materials Science and Engineering: B (Advanced Functional Solid-State Materials) 176, 1733-1740.

Wykrzykowska, J.J., Onuma, Y., Serruys, P.W., 2009. Advances in Stent Drug Delivery: the Future is in Bioabsorbable Stents. Expert Opinion on Drug Delivery 6, 113-126.

Zartner, P., Cesnjevar, R., Singer, H., Weyand, M., 2005. First Successful Implantation of a Biodegradable Metal Stent into the Left Pulmonary Artery of a Preterm Baby. Catheterization and Cardiovascular Interventions, 66, 590-594.